Title

Experimental Curative Fluorescence-guided Surgery of Highly Invasive Glioblastoma Multiforme Selectively Labeled With a Killer-reporter Adenovirus

Journal

Molecular Therapy, 23(7)

ISSN

1525-0016

Authors

Yano, Shuya
Miwa, Shinji
Kishimoto, Hiroyuki
et al.

Publication Date

2015-07-01

DOI

10.1038/mt.2015.63

Peer reviewed

Experimental Curative Fluorescence-guided Surgery of Highly Invasive Glioblastoma Multiforme Selectively Labeled With a Killer-reporter Adenovirus

Shuya Yano[1,2,3], Shinji Miwa[1,2], Hiroyuki Kishimoto[3], Makoto Toneri[1,2], Yukihiko Hiroshima[1,2], Mako Yamamoto[1,2], Michael Bouvet[2], Yasuo Urata[4], Hiroshi Tazawa[5], Shunsuke Kagawa[3], Toshiyoshi Fujiwara[3] and Robert M Hoffman[1,2]

[1]AntiCancer, Inc., San Diego, California, USA; [2]Department of Surgery, University of California San Diego, San Diego, California, USA; [3]Department of Gastroenterological Surgery, Okayama University, Graduate School of Medicine, Dentistry and Pharmaceutical Sciences, Okayama, Japan; [4]Oncolys BioPharm Inc., Tokyo, Japan; [5]Center for Innovative Clinical Medicine, Okayama University Hospital, Okayama, Japan

Fluorescence-guided surgery (FGS) of cancer is an area of intense current interest. However, although benefits have been demonstrated with FGS, curative strategies need to be developed. Glioblastoma multiforme (GBM) is one of the most invasive of cancers and is not totally resectable using standard bright-light surgery (BLS) or current FGS strategies. We report here a curative strategy for FGS of GBM. In this study, telomerase-dependent adenovirus OBP-401 infection brightly and selectively labeled GBM with green fluorescent protein (GFP) for FGS in orthotopic nude mouse models. OBP-401–based FGS enabled curative resection of GBM without recurrence for at least 150 days, compared to less than 30 days with BLS.

Received 19 January 2015; accepted 1 April 2015; advance online publication 19 May 2015. doi:10.1038/mt.2015.63

INTRODUCTION

Fluorescence-guided surgery (FGS) of cancer is an area of intense interest[1–23] and has shown benefit, but generally is not curative.[24–26]

Fluorescence-guided surgery has shown to have potential for highly invasive glioblastoma multiforme (GBM).[24–28] Treatment with the metabolite 5-aminolevulinic acid, a precursor of hemoglobin, resulted in the accumulation of porphyrins within malignant glioma.[24,25] Patients with malignant gliomas were given 5-aminolevulinic acid orally and then underwent FGS and had a greater percentage with apparent complete resection and longer 6-month progression-free rate compared to patients who underwent bright-light surgery (BLS).[24,25]

We previously compared FGS and BLS of red fluorescent protein (RFP)-expressing U87 human glioma orthotopically implanted in nude mice. Most glioma cells were removed by FGS. In contrast, the glioma was difficult to visualize under bright light, and many residual cancer cells remained in the brain after bright-light surgery. FGS significantly extended the survival of the mice compared to those who underwent BLS, but it was not curative.[29]

In an intraperitoneal mouse model of disseminated colon cancer, FGS enabled resection of all tumor nodules labeled with green fluorescent protein (GFP) by telomerase-dependent GFP-containing adenovirus, OBP-401.[30,31] We also observed that, in addition to labeling cancer cells, OBP-401 had cancer-cell killing efficacy.[30,31] OBP-401 should have activity for the vast majority of cancers since they would be expected to express telomerase.[32–38]

In this report, we investigated whether GFP labeling with OBP-401 could result in curative FGS of highly invasive GBM implanted orthotopically in nude mice.

RESULTS

GFP-expressing adenovirus OBP-401 labels GBM cells with GFP and subsequently kills them

We first confirmed whether OBP-401 labels glioblastoma (GBM) cells *in vitro* using the U87MG RFP-expressing GBM cell line. Time-lapse imaging showed that OBP-401 labeled RFP-expressing U87MG glioma cells with GFP in a dose-dependent manner (**Supplementary Figure S1**). Moreover, OBP-401 killed glioma cells in a dose-dependent manner (**Supplementary Figure S1**).

Orthotopic nude mouse model of GBM

RFP-expressing glioma tissue fragments grown subcutaneously in nude mice were implanted into the subdural space and sutured to the meninges for stabilization (**Figure 1** and **Supplementary Figure S2**). The orthotopic GBM invaded the brain tissue (**Figure 1**).

Bright-light surgery cannot fully resect GBM

The orthotopic glioma tumor invaded brain tissue and therefore the margin between the tumor and normal tissues was unclear under bright light (**Figure 2**). Radical surgery damaged the brain tissue and resulted in death. When only tumor was resected, residual disease remained visible by RFP expression (**Figure 3**).

Correspondence: Robert M Hoffman, AntiCancer, Inc, 7917 Ostrow Street, San Diego, California 92111, USA. E-mail: all@anticancer.com

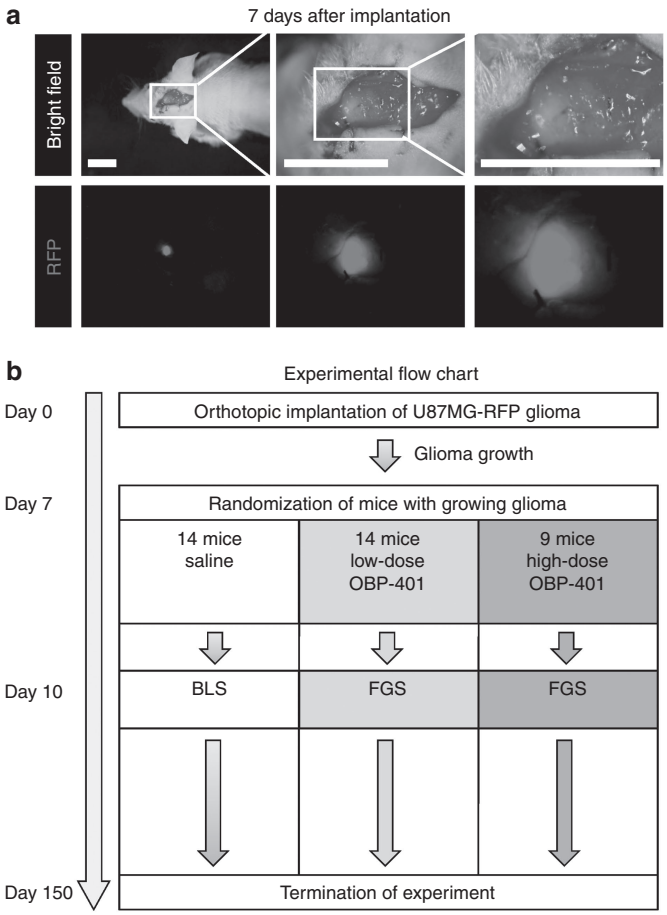

Figure 1 Orthotopic glioblastoma model. RFP-expressing U87MG cells (5×10^6), suspended in Matrigel, were inoculated into the right flank of 5-week-old female arthymic nude mice. After the tumor grew, it was harvested and cut into small pieces (2–3 mm). A craniotomy open window was made at the right parietal bone using a skin biopsy punch. The meninges was opened to place a small fragment of glioma tissue on the brain. The glioma tissue was sutured with an 8-0 nylon suture for stabilization. The RFP signal of the implanted tumor was visible outside the skin using a noninvasive whole-body fluorescence imaging system (OV100). (**a**) Representative images of orthotopic glioma model 7 after implantation at various magnifications (left panel = 10 mm; middle panel = 10 mm; right panel: 6 mm. (**b**) Experimental flowchart.

Low-dose OBP-401 GFP labeling of orthotopic glioma

Low-dose OBP-401 (1×10^8 plaque-forming unit [PFU]) was intaratumorally injected into the GBM 3 days before FGS. OBP-401 labeled the GBM with GFP (**Figure 2**). OBP-401 clearly highlighted the margin between the glioma and brain tissue (**Figure 2**). OBP-401 GFP labeling matched the RFP expression of the tumor (**Figure 2**).

OBP-401 FGS of GBM cells after BLS

Orthotopic glioma was resected with BLS 3 days after injection of low-dose OBP-401 (**Figure 3**). OBP-401 enabled detection of residual GBM cells after BLS (**Figure 3**). Residual GBM cells were removed with OBP-401 FGS with minimal resection (**Figure 3**). Tumor resected by BLS and subsequently by FGS had matched GFP and RFP expression. Confocal microscopy detected residual OBP-401-GFP-labeled GBM at the single-cell level (**Figure 3**).

GBM recurrence with low-dose OBP-401-FGS

The rate of local recurrence with low-dose (1×10^8 PFU) OBP-401 FGS and BLS alone was determined. Twelve of 14 mice that received BLS had large recurring RFP fluorescing tumors. In contrast, 5 of 14 mice that underwent OBP-401 FGS had small recurrent RFP tumors ($P = 0.007$). Low-dose OBP-401 FGS reduced the rate of local recurrence ($P = 0.002$), the volume of the recurrence ($P = 0.003$), and prolonged the survival rate after surgery, compared with BLS ($P = 0.0013$; **Figure 5**).

High-dose OBP-401 enables less invasive, recurrence-free FGS

High-dose administration of OBP-401 (2×10^8) PFU significantly reduced the size of the tumor compared with untreated control or low-dose OBP-401-treated tumor (mock versus low-dose FGS: $P < 0.05$; low-dose versus high-dose: $P < 0.05$; **Figure 4**). The glioma was much more effectively resected with high-dose OBP-401 FGS than with low-dose OBP-401 FGS or BLS. All mice which received high-dose FGS were alive at 150 days with no recurrence, significantly longer than low-dose OBP-401-FGS ($P = 0.05$) which was significantly better than BLS ($P = 0.002$); (**Figure 4**). High-dose OBP-401 also enabled a less extensive surgery to resect the tumor completely. Similar results were seen with overall survival, with high-dose OBP-401-FGS longer than low-dose OBP-401-FGS ($P = 0.05$) or BLS ($P < 0.01$); (**Figure 4**).

OBP-401 kills invading GBM cells

U87MG cells formed "spikes" of invading cells in monolayer culture (**Supplementary Figure S3**). OBP-401 reduced the number and length of the invading spikes (**Supplementary Figure S3**). RFP-expressing U87MG cells were also grown in three-dimensional Gelfoam histoculture. Time-lapse imaging showed that U87MG cells formed nodules and invaded outward along the structure of Gelfoam histoculture (**Figure 5**). Therefore, we were able to track invading and moving GBM cells in real-time by OBP-401 labeling. Time-lapse imaging showed that OBP-401 clearly labeled invading GBM cells in three-dimensional Gelfoam histoculture (data not shown), OBP-401 reduced the number and the distance of invading GBM cells (**Figure 5**). The killing of invading glioma cells by high-dose OBP-401 in Gelfoam can explain why high-dose OBP-401, in conjunction with FGS, can eliminate recurrence since invading glioma are probably eliminated by this procedure *in vivo*.

DISCUSSION

Conclusions and future prospects

Fluorescence-guided surgery has shown important potential for improving outcome.[1–24,29–31,39–41] OBP-301,[42–47] the parent virus of OBP-401, was well tolerated in a phase 1 clinical trial of patients with advanced cancer.[48] This trial suggest that OBP-301 and its derivative OBP-401 are safe. Previous results,[30,31,40] as well as the current study, have shown OBP-401 is cancer specific. The results

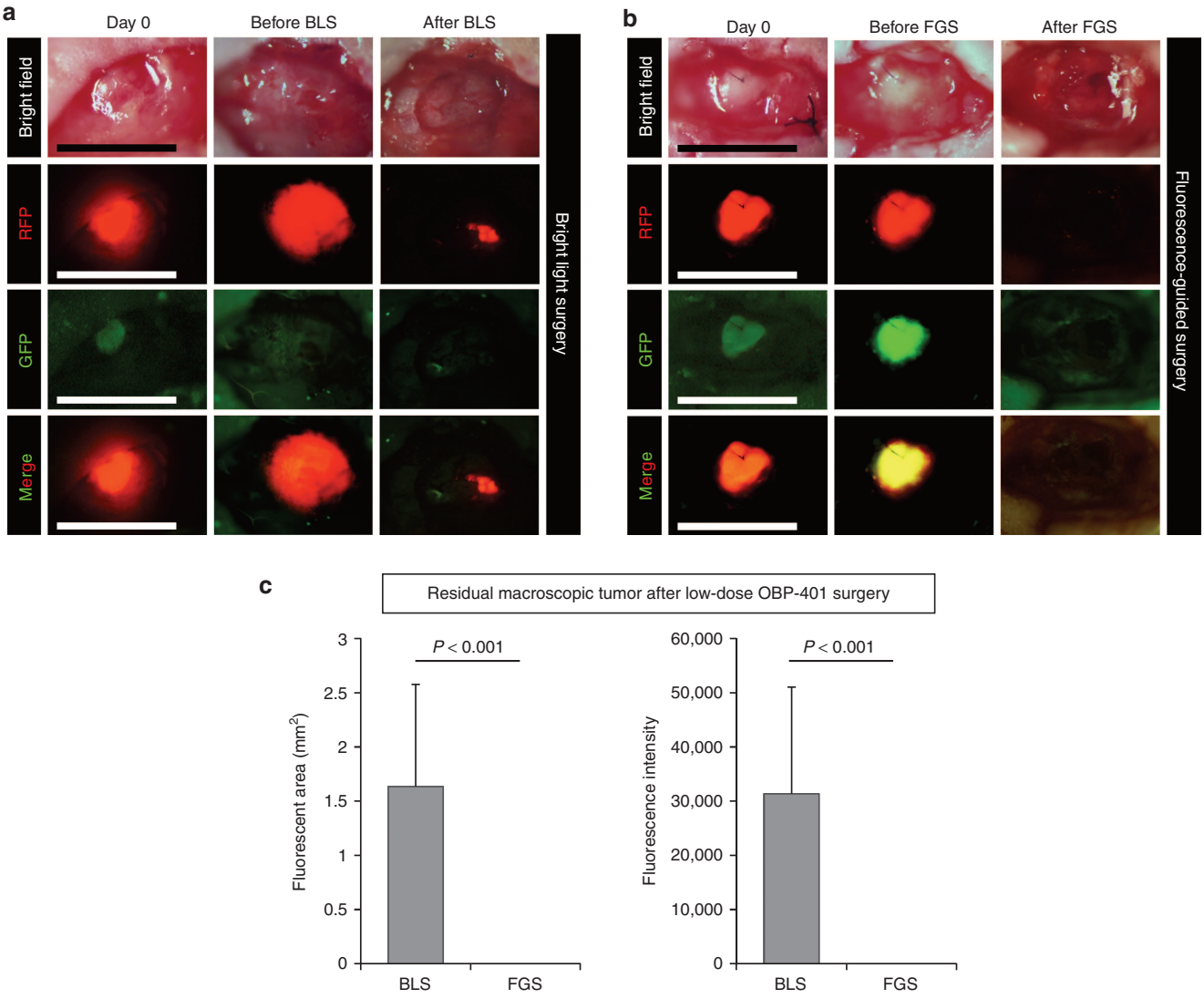

Figure 2 Comparison of low-dose OBP-401-based fluorescence-guided surgery (FGS) with bright-light surgery (BLS). For FGS, OBP-401 was injected intratumorally (1×10^8 PFU) when the tumors reached approximately 30 mm^3 (diameter; 4 mm). (**a**) Representative whole-tumor images of mock-infected orthotopic glioma before and after BLS. (**b**) Representative whole-tumor images of an orthotopic glioma before infection with OBP-401 and before and after OBP-401 FGS. (**c**) Histogram shows the comparison of fluorescent areas of residual tumor in the surgical bed after BLS or low-dose OBP-401 FGS ($P < 0.001$) (left). Fluorescent area is calculated with Image J software. Histogram shows the comparison of the fluorescence intensity of residual tumor in the surgical bed after BLS and low-dose OBP-401-FGS ($P < 0.001$) (right). The fluorescence intensity is calculated with Image J software. Data are shown as average ± SD. $n = 14$.

of the current study suggest that OBP-401 FGS has important translational clinical potential to improve resection and outcome of glioma without undue toxicity. OBP-401 has also shown promise for FGS of GI cancer.[30,40] Clinical trials of OBP-401 for these diseases are in order. Future studies may also exploit OBP-401 for suicide gene therapy of cancer.

MATERIALS AND METHODS

GFP-expressing telomerase-specific adenovirus. The recombinant GFP-expressing, telomerase-dependent, replication-competent adenovirus vector OBP-401 contains the promoter element of the human telomerase reverse transcriptase (*hTERT*) gene which drives the expression of the E1A and E1B genes linked to an internal ribosome entry site for selective replication in telomerase-expressing cancer cells. The *GFP* gene is driven by the CMV promoter.[30,31,49]

Cell culture. U87MG-RFP human glioma cells[2,29] were maintained and cultured in DMEM medium with 10% fetal bovine serum and 5% penicillin/streptomycin.

***OBP-401 infection of glioma cells* in vitro.** U87MG-RFP cells (2×10^5) were seeded and cultured in DMEM with 10% fetal bovine serum (FBS) on a six-well plate for two-dimensional culture. OBP-401 was added at a multiplicity of infection of 10, 20, or 30 one day after culture. Cell viability was determined 6 days after infection. U87MG cells were also cultured on Gelfoam in DMEM with 10% FBS for three-dimensional culture. OBP-401 was added at 1×10^8 or 2×10^8 PFU 2 days after the beginning of culture.

Mice. Athymic nude *nu*/*nu* mice (AntiCancer, San Diego, CA) were kept in a barrier facility under high-efficiency particulate arrestance filtration. Mice were fed with autoclaved laboratory rodent diet (Tecklad LM-485; Western Research Products, Orange, CA).

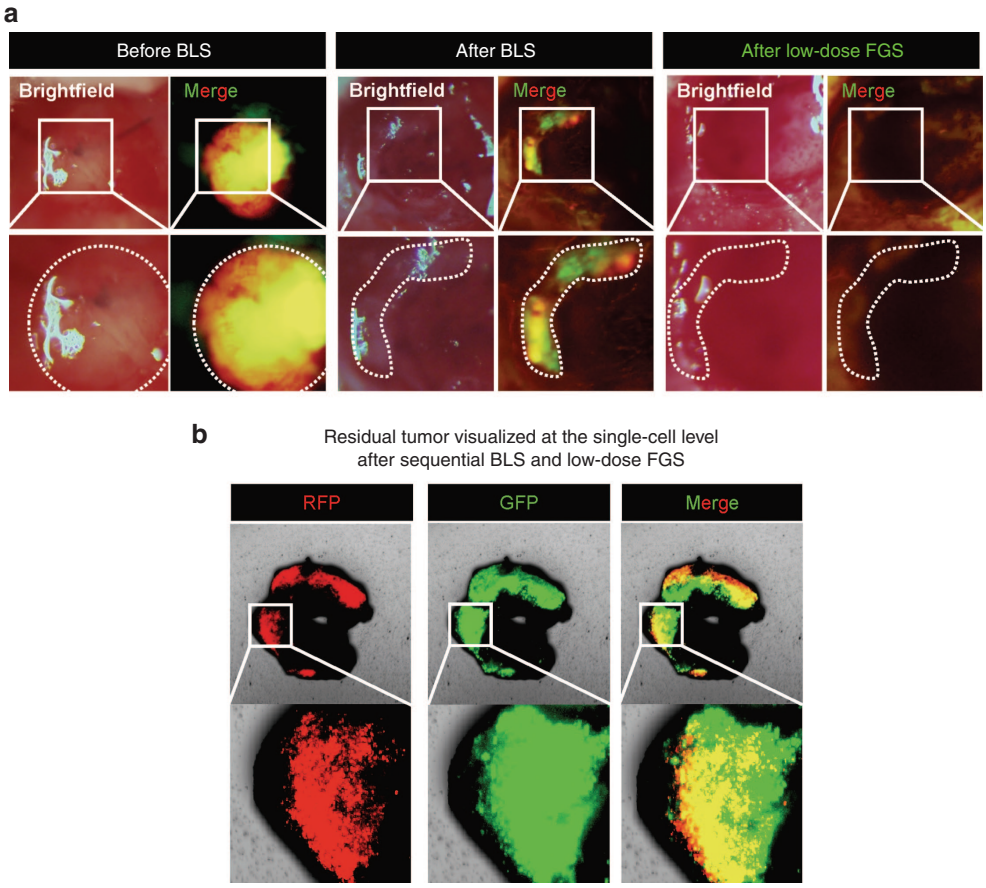

Figure 3 Low-dose OBP-401 visualizes residual glioma cells after BLS and FGS. OBP-401 was injected intratumorally (1×10^8 PFU) when the glioma reached ~30 mm^3. The GFP-labeled orthotopic glioma was resected by BLS, and then the residual tumor was resected by FGS. (**a**) Representative whole-tumor images of orthotopic glioma before and after BLS and after FGS. (**b**) Representative microscopic images, acquired with the FV1000 confocal laser scanning microscope, of residual glioma labeled with low-dose OBP-401-GFP after sequential BLS and FGS.

All animal studies were conducted in accordance with the principles and procedures outlined in the National Institutes of Health Guide for the Care and Use of Laboratory Animals under assurance A3873– 01.

Surgical orthotopic implantation glioma model. U87MG-RFP cells (5×10^6), suspended in Matrigel (40 µl), were inoculated into the right flank of 5-week-old female arthymic nude mice in order to obtain stock tumors. The resulting tumors were cut into small fragments (diameter: 2–3 mm). A craniotomy open window was made in the right parietal bone using a skin biopsy punch.[29,50] The meninges was opened to insert a fragment of GBP with 8-0 nylon suture.

In vivo *whole-body/whole-tumor imaging.* For whole-body or whole-tumor imaging, the OV100 Small Animal Imaging System (Olympus, Tokyo, Japan) was used.[51] The OV100 contained an MT-20 light source (Olympus Biosystems) and DP70 CCD camera (Olympus). High-resolution images were captured directly on a PC (Fujitsu Siemens, Munich, Germany). Images were processed for contrast and brightness and analyzed with the use of Paint Shop Pro 8 and CellR (Olympus Biosystems).[51]

Time-lapse images of OBP-401 labeling of GBM cells in two-dimensional culture or in Gelfoam histoculture were acquired with a confocal laser-scanning microscope (FV1000; Olympus) with two-laser diodes (473 and 559 nm). A 4×0.20 numerical aperture immersion objective lens (Olympus) was used. Scanning and image acquisition were controlled by Fluoview software (Olympus).[52]

OBP-401 based fluorescence-guided surgery. All animal procedures were performed under anesthesia using s.c. administration of a ketamine mixture (10 µl ketamine HCl, 7.6 µl xylazine, 2.4 µl acepromazine maleate, and 10 µl phosphate-buffered saline). OBP-401-GFP-labeled glioma was imaged with the OV100 to determine the resection area and margin, OBP-401-GFP-FGS was then performed with the OV100. When residual cancer cells remained after resection of the tumor, additional resection was performed. After all cancer cells were removed with OBP-401-GFP-FGS, the craniotomy was closed with 6-0 suture.

In vivo *single-cell level imaging of residual tumor.* Fluorescence images of residual tumor tissue after BLS or FGS were acquired using the FV1000 confocal microscope.

Statistical analysis. Data are shown as means ± SD. For comparison between two groups, significant differences were determined using the Student's *t*-test. For comparison of more than two groups, statistical significance was determined with a one-way analysis of variance (ANOVA) followed by a Bonferroni multiple-group comparison test. Pearson chi-square analysis was used to compare the rate of local recurrence between BLS and OBP-401 FGS. Recurrence is defined as the appearance of RFP fluorescence in the brain after BLS or FGS. Statistical analysis for disease-free survival, defined as time from FGS without recurrence, and overall survival, defined as time from FGS that mice are alive, was performed using the Kaplan–Meier test along with the log-rank test. Time of observation was 150 days and the curative end point is defined as no recurrence at 150 days. P values of ≤ 0.05 were considered significant.

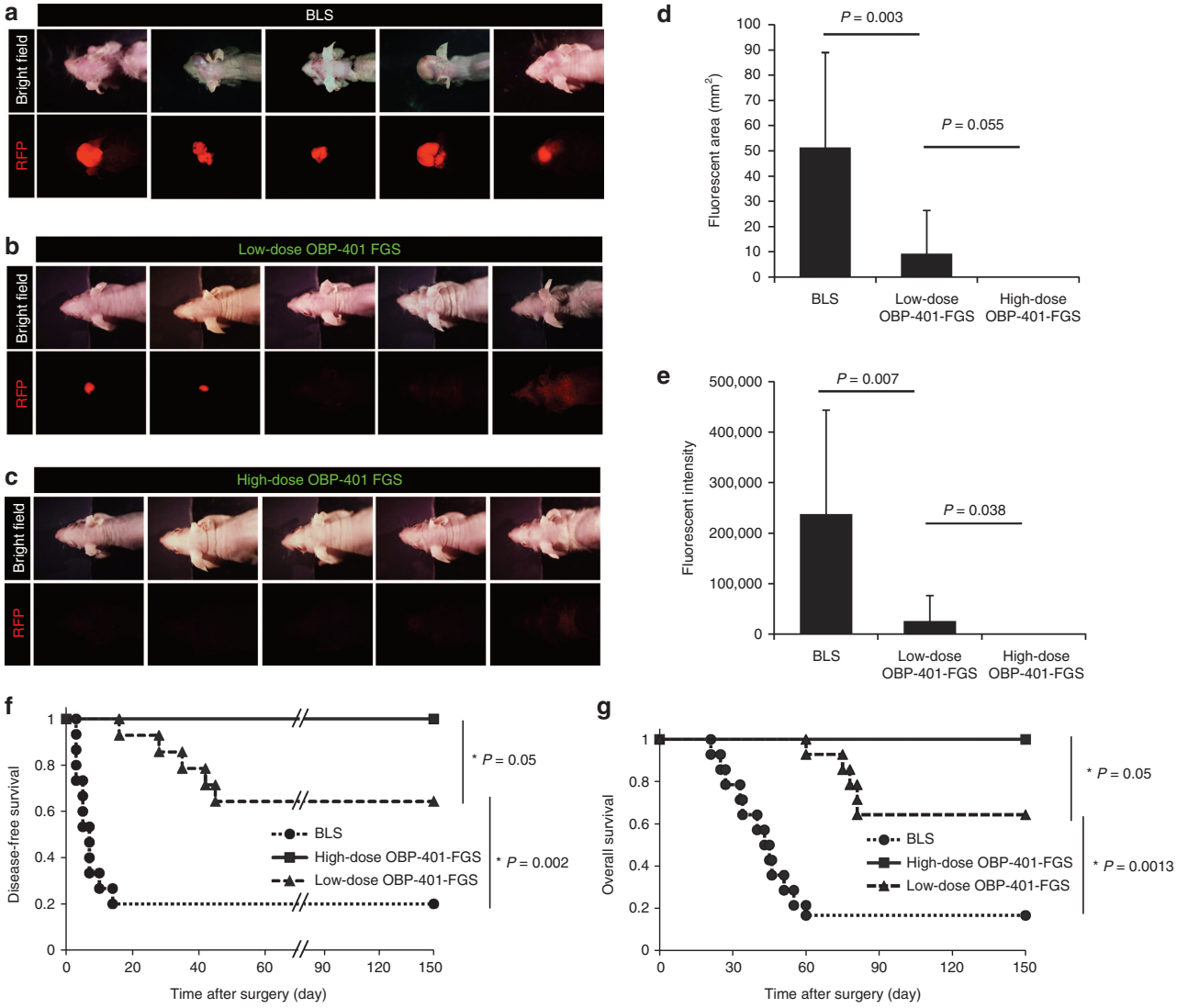

Figure 4 High-dose OBP-401–based FGS prevents local recurrence after surgery. (**a**) Representative whole-body images of five mice with orthotopic glioma 30–50 days after BLS. (**b**) Representative whole-body images of five mice with orthotopic glioma 70 days after low-dose OBP-401 FGS. (**c**) Representative whole-body images of orthotopic glioma 70 days after high-dose OBP-401 FGS. Bright-field (upper panels), RFP image (lower panels). (**d**) Comparison of fluorescent areas of recurrent tumors after BLS or low-dose OBP-401 FGS (BLS versus low-dose FGS; $P = 0.003$); or high-dose OBP-401 FGS (low-dose FGS versus high-dose FGS; $P = 0.055$). Fluorescent area is calculated with Image J software. (**e**) Comparison of fluorescence intensity of recurrent tumors after BLS or low-dose OBP-401 FGS (BLS versus low-dose FGS; $P = 0.007$) or high-dose OBP-401 FGS (low-dose FGS versus high-dose FGS; $P = 0.038$). Fluorescence intensity is calculated with Image J software. Data are shown as average ± SD. $n = 14$ (BLS); $n = 14$ (low-dose OBP-401-FGS); $n = 9$ (high-dose OBP-401-FGS). (**f**) Kaplan–Meier curve shows disease-free survival after BLS, low-dose OBP-401 FGS (BLS versus low-dose FGS; $P = 0.002$); or high-dose OBP-401 FGS (low-dose FGS versus high-dose FGS; $P = 0.05$). (**g**) Kaplan–Meier curve shows overall survival after BLS, low-dose OBP-401 FGS (BLS versus low-dose FGS; $P = 0.0013$); or high-dose OBP-401 FGS (low-dose FGS versus high-dose FGS; $P = 0.05$).

SUPPLEMENTARY MATERIAL

Figure S1. OBP-401 labels U87MG-RFP with GFP and then kills them *in vitro*.

Figure S2. Orthotopic glioblastoma model.

Figure S3. OBP-401 reduces invasion ability of human glioma cell line U87MG in monolayer in culture.

ACKNOWLEDGMENTS

This paper is dedicated to the memory of A. R. Moossa. This study was supported by grants-in-aid from the Ministry of Education, Science and Culture, Japan, and grants from the Ministry of Health and Welfare, Japan, and supported in part by National Cancer Institute grants CA132971 and CA142669.

Y.U. is President & CEO of Oncolys BioPharma, Inc., the manufacturer of OBP-401 (Telomescan). H.T. and T.F. are consultants of Oncolys BioPharma, Inc.

S.Y., T.F., and R.M.H. participated in conception and design of the study. S.Y., S.M., and H.K. helped in development of methodology. R.M.H., S.Y., and S.M. are responsible for acquisition of data (provided animals, provided facilities, etc.). S.Y., S.M., H.K., H.T., M.T., Y.H., M.Y., and R.M.H. conducted analysis and interpretation of data (e.g., statistical analysis, biostatistics, computational analysis). S.Y. and R.M.H. helped in writing, review, and/or revision of manuscript. R.M.H., H.K., H.T., T.F., and Y.U. provided administrative, technical, or material support. R.M.H., H.K., H.T., S.K., and T.F. helped in study supervision.

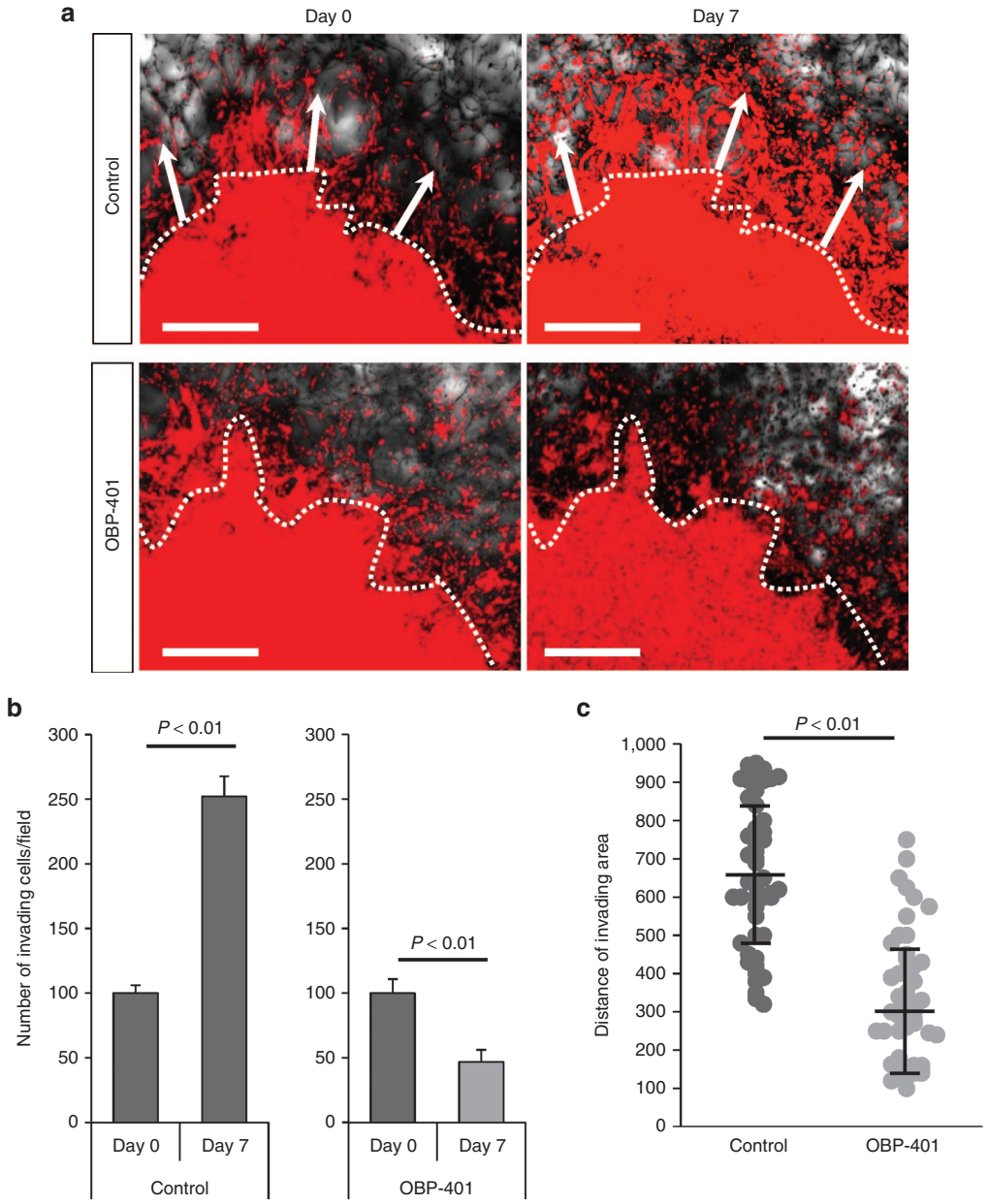

Figure 5 OBP-401 inhibits invading glioma cells and kills them in 3D Gelfoam histoculture. U87MG cells (5×10^6) expressing RFP, were seeded on Gelfoam for 3D histoculture. OBP-401 was added at 2×10^8 PFU 48 hours after seeding. All images were acquired with the FV1000 confocal laser scanning microscope. (**a**) Representative images from the RFP channel of mock-infected invading glioma cells (upper) and OBP-401-infected invading glioma cells (lower) cultured in Gelfoam histoculture. Dotted line separates invading area and tumor. Arrows show the direction of invading glioma cells. (**b**) Histogram shows the number of invading glioma cells for mock-infected and high-dose OBP-401-infected glioma cells in Gelfoam histoculture. (**C**) Scattergram shows the distance (μm) of invading glioma cells in Gelfoam histoculture from mock-infected glioma cells and high-dose OBP-401-infected glioma cells. Data are shown as average ± SD. $n = 5$.

REFERENCES

1. Bouvet, M and Hoffman, RM (2011). Glowing tumors make for better detection and resection. *Sci Transl Med* **3**: 110fs10.
2. Hoffman, RM (2005). The multiple uses of fluorescent proteins to visualize cancer in vivo. *Nat Rev Cancer* **5**: 796–806.
3. van Dam, GM, Themelis, G, Crane, LM, Harlaar, NJ, Pleijhuis, RG, Kelder, W *et al.* (2011). Intraoperative tumor-specific fluorescence imaging in ovarian cancer by folate receptor-α targeting: first in-human results. *Nat Med* **17**: 1315–1319.
4. Yamashita, S, Tokuishi, K, Miyawaki, M, Anami, K, Moroga, T, Takeno, S *et al.* (2012). Sentinel node navigation surgery by thoracoscopic fluorescence imaging system and molecular examination in non-small cell lung cancer. *Ann Surg Oncol* **19**: 728–733.
5. Eyüpoglu, IY, Hore, N, Savaskan, NE, Grummich, P, Roessler, K, Buchfelder, M *et al.* (2012). Improving the extent of malignant glioma resection by dual intraoperative visualization approach. *PLoS One* **7**: e44885.
6. Metildi, CA, Kaushal, S, Luiken, GA, Talamini, MA, Hoffman, RM and Bouvet, M (2014). Fluorescently labeled chimeric anti-CEA antibody improves detection and resection of human colon cancer in a patient-derived orthotopic xenograft (PDOX) nude mouse model. *J Surg Oncol* **109**: 451–458.
7. Metildi, CA, Kaushal, S, Hardamon, CR, Snyder, CS, Pu, M, Messer, KS *et al.* (2012). Fluorescence-guided surgery allows for more complete resection of pancreatic cancer, resulting in longer disease-free survival compared with standard surgery in orthotopic mouse models. *J Am Coll Surg* **215**: 126–35; discussion 135.
8. Ishizawa, T, Fukushima, N, Shibahara, J, Masuda, K, Tamura, S, Aoki, T *et al.* (2009). Real-time identification of liver cancers by using indocyanine green fluorescent imaging. *Cancer* **115**: 2491–2504.
9. Tran Cao, HS, Kaushal, S, Metildi, CA, Menen, RS, Lee, C, Snyder, CS *et al.* (2012). Tumor-specific fluorescence antibody imaging enables accurate staging laparoscopy in an orthotopic model of pancreatic cancer. *Hepatogastroenterology* **59**: 1994–1999.
10. Urano, Y, Sakabe, M, Kosaka, N, Ogawa, M, Mitsunaga, M, Asanuma, D *et al.* (2011). Rapid cancer detection by topically spraying a γ-glutamyltranspeptidase-activated fluorescent probe. *Sci Transl Med* **3**: 110ra119.

11. McElroy, M, Kaushal, S, Luiken, GA, Talamini, MA, Moossa, AR, Hoffman, RM *et al.* (2008). Imaging of primary and metastatic pancreatic cancer using a fluorophore-conjugated anti-CA19-9 antibody for surgical navigation. *World J Surg* **32**: 1057–1066.
12. Kaushal, S, McElroy, MK, Luiken, GA, Talamini, MA, Moossa, AR, Hoffman, RM *et al.* (2008). Fluorophore-conjugated anti-CEA antibody for the intraoperative imaging of pancreatic and colorectal cancer. *J Gastrointest Surg* **12**: 1938–1950.
13. Metildi, CA, Kaushal, S, Lee, C, Hardamon, CR, Snyder, CS, Luiken, GA *et al.* (2012). An LED light source and novel fluorophore combinations improve fluorescence laparoscopic detection of metastatic pancreatic cancer in orthotopic mouse models. *J Am Coll Surg* **214**: 997–1007.e2.
14. Metildi, CA, Kaushal, S, Hardamon, CR, Snyder, CS, Pu, M, Messer, KS *et al.* (2012**).** Fluorescence-guided surgery allows for more complete resection of pancreatic cancer, resulting in longer disease-free survival compared with standard surgery in orthotopic mouse models. *J Am Coll Surg* **215**: 126–135.
15. Metildi, CA, Kaushal, S, Snyder, CS, Hoffman, RM and Bouvet, M (2013). Fluorescence-guided surgery of human colon cancer increases complete resection resulting in cures in an orthotopic nude mouse model. *J Surg Res* **179**: 87–93.
16. Metildi, CA, Hoffman, RM and Bouvet, M (2013). Fluorescence-guided surgery and fluorescence laparoscopy for gastrointestinal cancers in clinically-relevant mouse models. *Gastroenterol Res Pract* **2013**: 290634.
17. Metildi, CA, Tang, CM, Kaushal, S, Leonard, SY, Magistri, P, Tran Cao, HS, *et al.* **(**2013**).** In vivo fluorescence imaging of gastrointestinal stromal tumors using fluorophore-conjugated anti-KIT antibody. *Ann Surg Oncol* **3**: 693–700.
18. Metildi, CA, Kaushal, S, Pu, M, Messer, KA, Luiken, GA, Moossa, AR *et al.* (2014). Fluorescence-guided surgery with a fluorophore-conjugated antibody to carcinoembryonic antigen (CEA), that highlights the tumor, improves surgical resection and increases survival in orthotopic mouse models of human pancreatic cancer. *Ann Surg Oncol* **21**: 1405–1411.
19. Hiroshima, Y, Maawy, A, Sato, S, Murakami, T, Uehara, F, Miwa, S *et al.* (2014). Hand-held high-resolution fluorescence imaging system for fluorescence-guided surgery of patient and cell-line pancreatic tumors growing orthotopically in nude mice. *J Surg Res* **187**: 510–517.
20. Hiroshima, Y, Maawy, A, Metildi, CA, Zhang, Y, Uehara, F, Miwa, S *et al.* (2014). Successful fluorescence-guided surgery on human colon cancer patient-derived orthotopic xenograft mouse models using a fluorophore-conjugated anti-CEA antibody and a portable imaging system. *J Laparoendosc Adv Surg Tech A* **24**: 241–247.
21. Metildi, CA, Kaushal, S, Luiken, GA, Hoffman, RM and Bouvet, M (2014). Advantages of fluorescence-guided laparoscopic surgery of pancreatic cancer labeled with fluorescent anti-carcinoembryonic antigen antibodies in an orthotopic mouse model. *J Am Coll Surg* **219**: 132–141.
22. Hiroshima, Y, Maawy, A, Zhang, Y, Sato, S, Murakami, T, Yamamoto, M *et al.* (2014). Fluorescence-guided surgery in combination with UVC irradiation cures metastatic human pancreatic cancer in orthotopic mouse models. *PLoS One* **9**: e99977.
23. Hiroshima, Y, Maawy, A, Zhang, Y, Murakami, T, Momiyama, M, Mori, R *et al.* (2014). Metastatic recurrence in a pancreatic cancer patient derived orthotopic xenograft (PDOX) nude mouse model is inhibited by neoadjuvant chemotherapy in combination with fluorescence-guided surgery with an anti-CA 19-9-conjugated fluorophore. *PLoS One* **9**: e114310.
24. Stummer, W, Pichlmeier, U, Meinel, T, Wiestler, OD, Zanella, F and Reulen, HJ; ALA-Glioma Study Group (2006). Fluorescence-guided surgery with 5-aminolevulinic acid for resection of malignant glioma: a randomised controlled multicentre phase III trial. *Lancet Oncol* **7**: 392–401.
25. Aldave, G, Tejada, S, Pay, E, Marigil, M, Bejarano, B, Idoate, MA *et al.* (2013). Prognostic value of residual fluorescent tissue in glioblastoma patients after gross total resection in 5-aminolevulinic Acid-guided surgery. *Neurosurgery* **72**: 915–20; discussion 920.
26. Senft, C, Bink, A, Franz, K, Vatter, H, Gasser, T and Seifert, V (2011). Intraoperative MRI guidance and extent of resection in glioma surgery: a randomised, controlled trial. *Lancet Oncol* **12**: 997–1003.
27. Wen, PY and Kesari, S (2008). Malignant gliomas in adults. *N Engl J Med* **359**: 492–507.
28. Kleihues, P, Louis, DN, Scheithauer, BW, Rorke, LB, Reifenberger, G, Burger, PC *et al.* (2002). The WHO classification of tumors of the nervous system. *J Neuropathol Exp Neurol* **61**: 215–25; discussion 226.
29. Momiyama, M, Hiroshima, Y, Suetsugu, A, Tome, Y, Mii, S, Yano, S *et al.* (2013). Enhanced resection of orthotopic red-fluorescent-protein-expressing human glioma by fluorescence-guided surgery in nude mice. *Anticancer Res* **33**: 107–111.
30. Kishimoto, H, Zhao, M, Hayashi, K, Urata, Y, Tanaka, N, Fujiwara, T *et al.* (2009). *In vivo* internal tumor illumination by telomerase-dependent adenoviral GFP for precise surgical navigation. *Proc Natl Acad Sci USA* **106**: 14514–14517.
31. Kishimoto, H, Kojima, T, Watanabe, Y, Kagawa, S, Fujiwara, T, Uno, F *et al.* (2006). *In vivo* imaging of lymph node metastasis with telomerase-specific replication-selective adenovirus. *Nat Med* **12**: 1213–1219.
32. Walsh, KM, Codd, V, Smirnov, IV, Rice, T, Decker, PA, Hansen, HM *et al.*; ENGAGE Consortium Telomere Group. (2014). Variants near TERT and TERC influencing telomere length are associated with high-grade glioma risk. *Nat Genet* **46**: 731–735.
33. Langford, LA, Piatyszek, MA, Xu, R, Schold, SC Jr and Shay, JW (1995). Telomerase activity in human brain tumours. *Lancet* **346**: 1267–1268.
34. DeMasters, BK, Markham, N, Lillehei, KO and Shroyer, KR (1997). Differential telomerase expression in human primary intracranial tumors. *Am J Clin Pathol* **107**: 548–554.
35. Hiraga, S, Ohnishi, T, Izumoto, S, Miyahara, E, Kanemura, Y, Matsumura, H *et al.* (1998). Telomerase activity and alterations in telomere length in human brain tumors. *Cancer Res* **58**: 2117–2125.
36. Hakin-Smith, V, Jellinek, DA, Levy, D, Carroll, T, Teo, M, Timperley, WR *et al.* (2003). Alternative lengthening of telomeres and survival in patients with glioblastoma multiforme. *Lancet* **361**: 836–838.
37. Huang, F, Kanno, H, Yamamoto, I, Lin, Y and Kubota, Y (1999). Correlation of clinical features and telomerase activity in human gliomas. *J Neurooncol* **43**: 137–142.
38. Harada, K, Kurisu, K, Tahara, H, Tahara, E, Ide, T and Tahara, E (2000). Telomerase activity in primary and secondary glioblastomas multiforme as a novel molecular tumor marker. *J Neurosurg* **93**: 618–625.
39. Kishimoto, H, Urata, Y, Tanaka, N, Fujiwara, T and Hoffman, RM (2009). Selective metastatic tumor labeling with green fluorescent protein and killing by systemic administration of telomerase-dependent adenoviruses. *Mol Cancer Ther* **8**: 3001–3008.
40. Kishimoto, H, Aki, R, Urata, Y, Bouvet, M, Momiyama, M, Tanaka, N *et al.* (2011). Tumor-selective, adenoviral-mediated GFP genetic labeling of human cancer in the live mouse reports future recurrence after resection. *Cell Cycle* **10**: 2737–2741.
41. Yano, S, Miwa, S, Kishimoto, H, Uehara, F, Tazawa, H, Toneri, M, *et al.* **(**2015**).** Targeting tumors with a killer-reporter adenovirus for curative fluorescence-guided surgery of soft-tissue sarcoma. *Oncotarget*, in press.
42. Kojima, T, Hashimoto, Y, Watanabe, Y, Kagawa, S, Uno, F, Kuroda, S *et al.* (2009). A simple biological imaging system for detecting viable human circulating tumor cells. *J Clin Invest* **119**: 3172–3181.
43. Kuroda, S, Fujiwara, T, Shirakawa, Y, Yamasaki, Y, Yano, S, Uno, F *et al.* (2010). Telomerase-dependent oncolytic adenovirus sensitizes human cancer cells to ionizing radiation via inhibition of DNA repair machinery. *Cancer Res* **70**: 9339–9348.
44. Kojima, T, Watanabe, Y, Hashimoto, Y, Kuroda, S, Yamasaki, Y, Yano, S *et al.* (2010). *In vivo* biological purging for lymph node metastasis of human colorectal cancer by telomerase-specific oncolytic virotherapy. *Ann Surg* **251**: 1079–1086.
45. Sasaki, T, Tazawa, H, Hasei, J, Kunisada, T, Yoshida, A, Hashimoto, Y *et al.* (2011). Preclinical evaluation of telomerase-specific oncolytic virotherapy for human bone and soft tissue sarcomas. *Clin Cancer Res* **17**: 1828–1838.
46. Tazawa, H, Yano, S, Yoshida, R, Yamasaki, Y, Sasaki, T, Hashimoto, Y *et al.* (2012). Genetically engineered oncolytic adenovirus induces autophagic cell death through an E2F1-microRNA-7-epidermal growth factor receptor axis. *Int J Cancer* **131**: 2939–2950.
47. Yano, S, Tazawa, H, Hashimoto, Y, Shirakawa, Y, Kuroda, S, Nishizaki, M *et al.* (2013). A genetically engineered oncolytic adenovirus decoys and lethally traps quiescent cancer stem-like cells in S/G2/M phases. *Clin Cancer Res* **19**: 6495–6505.
48. Nemunaitis, J, Tong, AW, Nemunaitis, M, Senzer, N, Phadke, AP, Bedell, C *et al.* (2010). A phase I study of telomerase-specific replication competent oncolytic adenovirus (telomelysin) for various solid tumors. *Mol Ther* **18**: 429–434.
49. Umeoka, T, Kawashima, T, Kagawa, S, Teraishi, F, Taki, M, Nishizaki, M *et al.* (2004). Visualization of intrathoracically disseminated solid tumors in mice with optical imaging by telomerase-specific amplification of a transferred green fluorescent protein gene. *Cancer Res* **64**: 6259–6265.
50. Momiyama, M, Suetsugu, A, Kimura, H, Chishima, T, Bouvet, M, Endo, I *et al.* (2013). Dynamic subcellular imaging of cancer cell mitosis in the brain of live mice. *Anticancer Res* **33**: 1367–1371.
51. Yamauchi, K, Yang, M, Jiang, P, Xu, M, Yamamoto, N, Tsuchiya, H *et al.* (2006). Development of real-time subcellular dynamic multicolor imaging of cancer-cell trafficking in live mice with a variable-magnification whole-mouse imaging system. *Cancer Res* **66**: 4208–4214.
52. Uchugonova, A, Zhao, M, Weinigel, M, Zhang, Y, Bouvet, M, Hoffman, RM *et al.* (2013). Multiphoton tomography visualizes collagen fibers in the tumor microenvironment that maintain cancer-cell anchorage and shape. *J Cell Biochem* **114**: 99–102.